Quantum study of the spin wave spectrum of a superlattice with ferromagnetic interfacial coupling

1992 J. Phys.: Condens. Matter 4 5001

(http://iopscience.iop.org/0953-8984/4/21/016)

J. Phys.: Condens. Matter 4 (1992) 5001–5014. Printed in the UK

Quantum study of the spin wave spectrum of a superlattice with ferromagnetic interfacial coupling

B Martínez† and R E Camley‡

† Instituto de Ciencia de Materiales de Barcelona, CSIC, Campus Universitad Autonoma de Barcelona, Bellaterra 08193, Spain

‡ Department of Physics, University of Colorado, Colorado Springs, Colorado 80907, USA

Received 5 August 1991, in final form 30 January 1992

Abstract. In this paper we have carried out a quantum study of the features of the spin wave spectrum of a superlattice composed of alternating layers of two different ferromagnetic materials or a ferromagnetic material and a non-magnetic material, with a ferromagnetic coupling at the interfaces. Depending on the intensity of the interactions in the interfaces and on the layer thickness very different types of thermal behaviour of the magnetization can be obtained. In the case of the ferromagnetic–non-magnetic system a clear tendency to a bidimensional type of behaviour is shown when the exchange coupling at the interfaces is very small, and a clear dependence of the thermal demagnetization on the layer thickness is observed. In the case of the system composed of two different ferromagnetic materials, in the weak-coupling limit at the interfaces, we observe a more rapid decrease of the magnetization with temperature for thinner unit cells. The opposite type of behaviour is observed in the strong-coupling limit.

1. Introduction

The term 'superlattice' is used to denote a regularity in a physical quantity (charge density, spin density, etc) which has a larger period than the period of the microscopic unit cell. The progress of evaporation techniques in recent years has made it possible to control the layer thickness at the atomic scale and to fabricate artificial superlattices.

Superlattices are interesting mainly from the following two viewpoints:

(i) as a model system for basic research;
(ii) as new materials that can only be obtained artificially.

Since superlattices are fabricated artificially we can design the structure of the samples in such a way as to study a specified problem or to magnify a desired property. Among other interesting problems, superlattices are very suitable systems for studying the magnetic properties of ultrathin films, surface effects and periodicity effects. From an experimental point of view a considerable number of papers have been published on the magnetic properties of different multilayered systems (Ni/Cu [1], Fe/V [2], Fe/Si [3], Cu/Mn [4], etc). On the other hand, early theoretical papers on magnetic excitations in superlattices were focused mostly on the magnetostatic modes. A calculation of the magnon energies for the propagation direction parallel

0953-8984/92/215001+14$04.50

to the surface of the superlattice and perpendicular to the magnetization was given by Grünberg and Mika [5]. Different calculations for general propagation directions have been performed by Camley *et al* [6, 7]. Camley and Cottam [8] have considered antiferromagnetic and ferromagnetic superlattices. Other papers have considered exchange effects. Albuquerque *et al* [9] studied the spin wave spectrum of a superlattice of two different materials using Bloch's equations and the transfer matrix method. Dobrzynski *et al* [10] considered only exchange effects in a system composed of two different ferromagnetic materials in the framework of the Heisenberg model, obtaining in closed form the bulk and surface magnetic Green functions for a superlattice system. Morkowski and Szajek [11] performed a study of the spin wave spectrum in a system with periodically modulated exchange integrals. An extensive study of a superlattice of two alternating ferromagnetic materials based on an inhomogeneous Ginzburg–Landau functional, including the temperature dependence of the magnetization and the spin dynamics using a generalized Bloch equation, has been performed by Schwenk *et al* [12].

Previous studies of $M(T)$ in superlattice structures have concentrated on the low-temperature regime. In this case the dispersion relation in the small-K limit can be written in the form $\omega = DK^2 + D'q^2$, where q is the Bloch wavevector perpendicular to the layers. As a result the magnetization decreases as a function of temperature in a similar fashion to the decrease in bulk materials, that is $M(T) = B'T^{3/2}$. B' is different from the value in the bulk materials and reflects the superlattice structure to some degree, that is the dispersion relation in the small-wavevector limit is different in the superlattice as compared with the bulk. Of course in the superlattice the artificial periodicity introduces gaps in the dispersion relation as well as changes in the small-wavevector dispersion relation. In contrast to previous work, our results focus on the changes in $M(T)$ introduced by the gaps and the effects of the external applied field. In addition to changes in B' we find that the gaps can significantly change the power law for the decrease in magnetization with temperature. Thus if one measures $M(T)$ above the low-temperature limit, one apparently obtains a decrease in magnetization of the form $M(T) = B'T^{\alpha}$. For the examples we have considered we found α can range from about 1.2 to 1.6 when no field is applied.

In the present paper we shall discuss the properties of the spin wave spectrum of two different superlattice systems. In the first case the superlattice is made up of alternating films of ferromagnetic and non-magnetic materials. The ferromagnetic film is arranged in a simple cubic structure. For the purposes of numerical calculations the ferromagnetic materials will be considered to have a moment of $S = \frac{5}{2}$ and an exchange integral $J = 27.6 \times 10^{-16}$ erg. The non-magnetic material layer thickness is taken into account by means of J_1; this parameter governs the exchange interactions between two consecutive films of ferromagnetic material.

In the second case studied the superlattice is composed of alternating films of two different ferromagnetic materials (hereafter referred to as materials 1 and 2), both arranged in a simple cubic structure. The characteristics of each material are taken into account by means of the corresponding moments, S_1 and S_2, and the exchange integrals, J_1 and J_2. For the purposes of numerical calculations the values chosen for these parameters are $S_1 = \frac{3}{2}$, $S_2 = \frac{5}{2}$, $J_1 = 14.19 \times 10^{-16}$ erg and $J_2 = 27.6 \times 10^{-16}$ erg.

The interaction in the interface between the materials is taken to be ferromagnetic and its value is gauged by means of the parameter J_I ($J_1 < J_I < J_2$). The coordinate system is constructed so that the Y-axis is perpendicular to the interfaces between the

different films. The external applied field H, is directed parallel to the superlattice plane in the Z-direction. The collective magnetic excitations of the system will be investigated as a function of the layer thickness and the intensity of the interface exchange interaction as well as the temperature and the external applied field.

2. Theory

As we have mentioned above we shall study firstly a superlattice system made up of alternating films of ferromagnetic and non-magnetic materials. The ferromagnetic material is arranged in a simple cubic structure. We shall consider that exchange interactions are dominant so we shall neglect dipolar interactions, furthermore we shall take into account nearest-neighbour interactions only.

The magnetic behaviour of the system is described by a Heisenberg-type Hamiltonian plus a Zeeman term that takes into account the interaction with the external applied field:

$$\mathcal{H} = -\tfrac{1}{2}\sum_{ij} J_{ij}\boldsymbol{S}_i \cdot \boldsymbol{S}_j - g\mu_B \boldsymbol{H}\sum_i S_i^Z. \tag{1}$$

Here the sum in the first term is over the sites i and the nearest neighbours j, $\boldsymbol{H}$ is a static external field directed along the Z-axis and $\boldsymbol{S}$ is the spin angular momentum operator. By using the raising, S^+, and lowering, S^-, spin operators the Hamiltonian takes the following form in the absence of a magnetic field:

$$\mathcal{H} = -\sum_{ij} J_{ij}[\tfrac{1}{2}(S_i^+ S_j^- + S_i^- S_j^+) + S_i^Z S_j^Z]. \tag{2}$$

To proceed it is convenient to introduce the boson creation and annihilation operators $a_i^\dagger$ and a_i, respectively, defined by the well known Holstein–Primakoff transformation [13], which is given by the following relations:

$$\begin{aligned} S_{iZ} &= S - a_i^\dagger a_i \\ S_i^- &= (2S)^{1/2} a_i^\dagger (1 - a_i^\dagger a_i/2S)^{1/2} \\ S_i^+ &= (2S)^{1/2}(1 - a_i^\dagger a_i/2S)^{1/2} a_i. \end{aligned} \tag{3}$$

Finally another transformation from the atomic operators $a_i^\dagger$, a_i to the magnon variables $a_K^\dagger$, a_K is made. Spin waves could be introduced in this way by the following Fourier expansion [14] in terms of the wavevectors $\boldsymbol{K}$,

$$a_K^\dagger = \frac{1}{\sqrt{N}}\sum_j a_j^\dagger \exp(-\mathrm{i}\boldsymbol{K}\cdot\boldsymbol{R}_j) \qquad a_K = \frac{1}{\sqrt{N}}\sum_j a_j \exp(\mathrm{i}\boldsymbol{K}\cdot\boldsymbol{R}_j) \tag{4}$$

where $\boldsymbol{R}_j$ is the position vector of the atom j and N is the total number of spins. When the transformation defined by (3) is introduced in (2) a very complex expression is obtained. Usually the following approximations are considered [15]:

(i) at low temperatures the condition of quasi-saturation is invoked so that $(1 - a_i^\dagger a_i/2S)^{1/2} \simeq 1$;

(ii) neglect terms proportional to $a_i^\dagger a_i a_j^\dagger a_j$ because no correlation in the location of the different spin deviations is assumed;

(iii) terms proportional to $(2S)^{1/2} a_i^\dagger a_i a_j^\dagger$ are neglected because they are claimed to be smaller than the terms retained by the ratio $\langle a_i^\dagger a_i \rangle / (2S)^{1/2}$.

After carrying out these approximations the Hamiltonian of the system takes the following expression:

$$\mathcal{H} = C_1 g\mu_B H \sum_l a_l^\dagger a_l - \tfrac{1}{2} S \sum_{ij} J_{ij} (a_i^\dagger a_j - a_i^\dagger a_i). \tag{5}$$

Once we have arrived at this point we shall discuss the construction of the Hamiltonian of the superlattice system made up of alternating films of ferromagnetic and non-magnetic materials (see figure 1).

For a spin located in the monatomic layer a the Hamiltonian should be

$$\mathcal{H} = -J\,[S_a \cdot S_a(1 + \delta) + S_a \cdot S_b] - g\mu_B H S_a^Z. \tag{6}$$

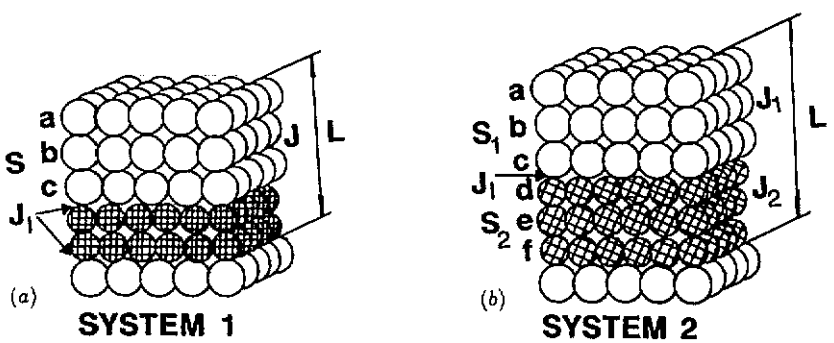

Figure 1. (*a*) Scheme of the unit cell of the superlattice for system 1 showing the different monatomic layers of magnetic material. (*b*) The same scheme for system 2.

The final term of the right-hand side stands for the Zeeman interaction with the external field. The term $S_a \cdot S_a(1 + \delta)$ takes into account the interactions of the atom located at the position l with its four nearest neighbours located in the same monatomic layer a, while the term $S_a \cdot S_b$ reflects the interaction with the nearest neighbour located in the monatomic layer b.

In order to analyse the contribution of the $S_a \cdot S_a(1 + \delta)$-type terms we should have in mind the simple cubic structure of the material and the transformation given by the relations (2), (3) and a two-dimensional Fourier transformation (in the plane of the spins) similar to equation (4). In so doing, after some algebra, it is possible to arrive at the following expression:

$$JS_a \cdot S_a(1 + \delta) = JS \sum_K [4 - 2(\cos K_X a + \cos K_Z a)] a_K^\dagger a_K. \tag{7}$$

Here a is the lattice parameter of the simple cubic atomic cell and K_X and K_Z are the X- and Z-components of the wavevector K.

Similarly, the evaluation of the $S_a \cdot S_b$-type terms leads to the following expression:

$$JS_a \cdot S_b = JS \sum_K \left(-a_K^\dagger a_K - b_K^\dagger b_K + a_K^\dagger b_K + b_K^\dagger a_K \right). \tag{8}$$

Here $a_K^\dagger a_K$ and $b_K^\dagger b_K$ are the creation and annihilation operators acting on the spins located in the monatomic layers a and b, respectively.

The contribution arising from the Zeeman interaction with the external applied field of intensity H directed along the Z-axis is given by the expression:

$$g\mu_B H S_a^Z = Sg\mu_B H \sum_i a_i^\dagger a_i = Sg\mu_B H \sum_K a_K^\dagger a_K. \tag{9}$$

The contribution to the Hamiltonian of the superlattice arising from the spins located in the monatomic layer a is given by the expressions (7), (8) and (9). The contribution of the remaining monatomic layers of the unit cell can be obtained easily in the same way. We shall comment briefly on the case of the last monatomic layer of the unit cell (layer c in figure 1). In this case the interaction with the spin located in the lower layer should be with the spin located in the layer a′ belonging to the following unit cell. Furthermore between layers c and a′ we have a film of non-magnetic material, so the intensity of the interaction between both spins is gauged by J_I instead of J.

The monatomic layer a′ is related with the monatomic layer a by means of the periodicity conditions. The creation and annihilation operators $a'^\dagger$, a' are related with $a^\dagger$, a by means of the Bloch theorem:

$$a' = a e^{iq \cdot L} \qquad a'^\dagger = a^\dagger e^{-iq \cdot L} \tag{10}$$

where L is the length of the unit cell of the superlattice and q is the wavevector in the Y-direction. By using relation (10) the term of the interaction between the layers c and a′ could be written in the following way:

$$J_I S_c \cdot S_{a'} = J_I S \sum_K \left(c_K^\dagger a_K e^{iq \cdot L} + a_K^\dagger c_K e^{-iq \cdot L} - c_K^\dagger c_K - a_K^\dagger a_K \right). \tag{11}$$

Once we have arrived at this point we can formulate the Hamiltonian of the superlattice collecting all the preceding terms. The Hamiltonian is an $N \times N$ complex matrix, N being the number of monatomic layers in the unit cell. The following step is to diagonalize the Hamiltonian; the eigenvalues obtained in this way are nothing but the vibrational modes of the spin network which are directly related with the Bose–Einstein occupation factors through the following expression:

$$\alpha_{qK}^\dagger \alpha_{qK} = \eta_{qK} = [\exp(\hbar\omega_{qK}/k_B T) - 1]^{-1}. \tag{12}$$

Expression (12) gives the average value of the number of magnons excited in the mode (q, K), where q, K are the wavevectors in the directions perpendicular and parallel to the superlattice. The total number of magnons excited at a temperature T is obtained by summing the contributions of all the modes. To carry out this summation we make use of the periodicity of the superlattice in q and the periodicity of the cubic lattice in K. Using the Fourier expansion given by (4) and after some algebra

it is possible to show that the summation over all the modes can be transformed in a summation over q and K,

$$\langle \eta \rangle = \frac{V}{(2\pi)^3} \int_{\pi/L}^{\pi} \int_{\pi/L}^{\pi} \int_{0}^{\pi} \mathrm{d}K_X \, \mathrm{d}K_Z \, \mathrm{d}q \, [\exp(\hbar\omega_{qK}/k_B T) - 1]^{-1} \tag{13}$$

where the integration was carried out in the first Brillouin zone by using 5×10^5 points in reciprocal space.

In regard to how we remove the singularity at zero frequency ($q = 0, K = 0$) we use an old trick, which was suggested and described by Klein and Smit [16]. Essentially we consider a finite-sized crystal with fixed end boundary conditions rather than periodic boundary conditions. This means there is no $\omega = 0$ state, but a state very close by at $K = \pi/L$. As shown in [16] this dependence on the size of the crystal (through L) is very weak and we have checked that for reasonable values of L we obtain the proper bulk behaviour for thick films. Recent treatments [17] have also shown how anisotropy fields or the dipolar fields can remove the singularity at $\omega = 0$. The accuracy of the numerical integration was checked by changing the number of points. A calculation of the thermal demagnetization of bulk iron was also carried out and a slope of 1.50 was obtained in the $\ln(\Delta M/M)$ against $\ln(T)$ plot. The magnetization at temperature T is given by

$$M(T)/M(T=0) = 1 - [\langle \eta \rangle / S_{\text{Total}}] \tag{14}$$

where S_{Total} is a normalization factor over the total spin of the unit cell.

In the case of system 2 involving two different magnetic materials the construction of the Hamiltonian is completely similar to the case mentioned above. Some care must be taken when the contribution of the spins located at the interfaces of both materials is formulated. For the sake of clarity we shall write out these terms explicitly. Making reference to figure 1 the term that takes into account the interaction between the monatomic layers c and d is given by

$$J_I S_c \cdot S_d = J_I \sum_K [-S_2 c_K^\dagger c_K - S_1 d_K^\dagger d_K + (S_1 S_2)^{1/2} (c_K^\dagger d_K + d_K^\dagger c_K)] \tag{15}$$

where J_I is the exchange integral between both materials, S_1 and S_2 are the values of the spin angular momenta for materials A and B, respectively.

The interaction of a spin located in the monatomic layer f with the corresponding spin in the layer a′ that belongs to the next unit cell is given by

$$J_I S_f \cdot S_{a'} = J_I \sum_K [-S_1 f_K^\dagger f_K - S_2 a_K^\dagger a_K + (S_1 S_2)^{1/2} (f_K^\dagger a_K e^{iq\cdot L} a_K^\dagger f_K e^{-iq\cdot L})] \tag{16}$$

where we have used the Bloch theorem given by relations (10).

3. Results

We shall consider first the low-temperature magnetization properties. In a bulk uniform sample the magnetization should decrease according to Bloch's law

$$M(T)/M(0) = 1 - BT^{3/2}. \tag{17}$$

Except for very thin samples this result is independent of the sample size [16], but in a superlattice the situation can be quite different. As usual the low-temperature magnetization depends on the spin wave spectrum. The spin waves of the superlattice will differ substantially from those in the bulk samples of the individual materials in two respects.

(i) The periodicity of the superlattice introduces gaps into the spin wave spectrum. These gaps allow the spin wave frequencies to differ considerably from the $\omega = DK^2$ dispersion law for bulk materials. Thus the magnetization can also deviate from the $T^{3/2}$ law.

(ii) The interface exchange interaction can be quite different from the exchange constant in each of the constituent films. For small wavevectors q, perpendicular to the layers, the dispersion relation will be approximately given by $\omega = D_{\text{eff}}q^2$, where D_{eff} depends on the exchange constants in materials A and B (J_1 and J_2), the magnitude of the spins (S_1 and S_2) and the interface exchange constant J_{I}.

For very thin ferromagnetic layers the interface exchange constant can play a significant role in determining D_{eff}. While D_{eff} does not change the 3/2-power law, it governs the size of the coefficient B in Bloch's $T^{3/2}$ law, with a large value of D_{eff} leading to a small value of the coefficient B.

From the diagonalization of the Hamiltonian we found the net spin deviation for each excitation and then performed a thermal average to find the change in magnetization as a function of the temperature. We note that care must be taken in the thermal average to avoid non-physical singularities [16].

3.1. Systems of ferromagnetic and non-magnetic materials

In the first case we have studied the thermal behaviour of a superlattice containing alternating films of magnetic and non-magnetic materials. As we have mentioned above, for the purpose of numerical calculations we have taken $S = 5/2$ and $J = 27.6 \times 10^{-16}$ erg, and the study has been performed as a function of the number of monatomic layers in the unit cell and the strength of the exchange interaction J_{I} between two consecutive magnetic films across the non-magnetic film.

3.1.1. Weak coupling. In this limit we have taken the value of J_{I} to be 10^{-17} erg ($J_{\text{I}} \ll J$), which is appropriate for a thick layer of non-magnetic spacer material.

In figure 2 we show the thermal behaviour of the magnetization as a function of the thickness of the magnetic film. It is evident from the figure that the system has a clear tendency to behave as a bidimensional ferromagnet, that is the decrease in $M(T)$ over the entire temperature range looks closer to a linear law than to a $T^{3/2}$ power law. This type of behaviour is more evident as the number of layers of the unit cell decreases and the system deviates clearly from the $T^{3/2}$ power law (see figure 3). Nevertheless, if we change the range of temperatures we observe a variation of the exponent that is more evident as the thickness of the magnetic film decreases. This type of behaviour is also shown in figure 3. We have performed a complete study of the evolution of the exponent, varying the range of temperatures over which the thermal demagnetization is considered. We observe that even in the case of the thinnest magnetic layer the system exhibits a Bloch law type of behaviour provided we consider only very low temperatures, (namely 0.1 to 1 K). As we increase

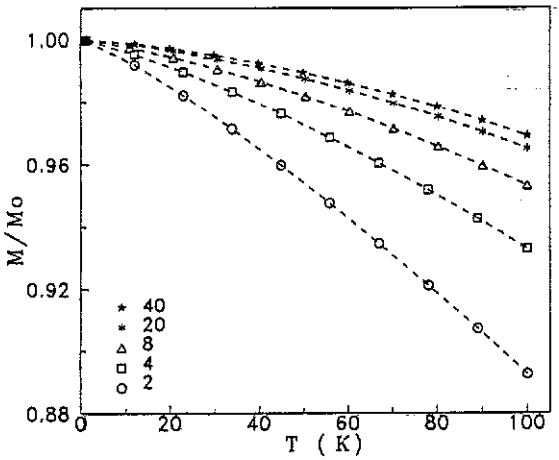

Figure 2. Thermal behaviour of the magnetization as a function of the thickness of the unit cell (in monatomic layers). The value of J_1 is 10^{-17} erg and the external applied field is zero.

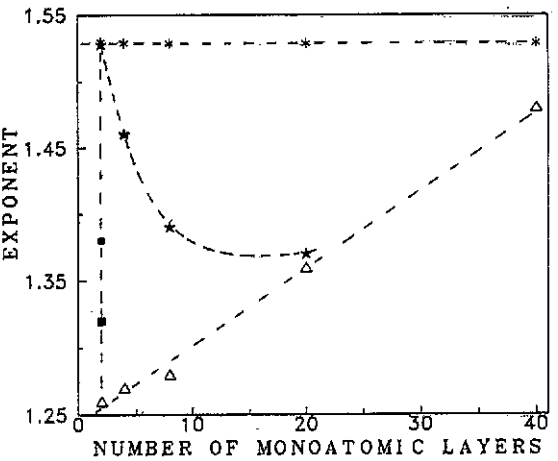

Figure 3. Variation of the exponent of the '$T^{3/2}$ power law' as a function of the thickness of the unit cell. Strong-coupling limit for $T \leqslant 30$ K, *. Weak-coupling limit for $T \leqslant 1$ K, *; $T \leqslant 5$ K, ●; $T \leqslant 10$ K, ■; $T \leqslant 100$ K, Δ.

the range of temperatures over which the thermal demagnetization is considered the exponent changes from 1.53 to 1.25.

This effect may be explained by taking into account the magnon band structure of the superlattice. As the number of layers of the unit cell decreases the effect of the gaps becomes more important because they are larger and the distortion of the bands from the parabolic form extends over a wider range of the reduced Brillouin zone. This deviation from the parabolic form of the bands is reflected by a variation of the exponent of the $T^{3/2}$ power law.

As the range of temperature increases the number of gaps involved in the thermal population of the magnon bands increases as well and a larger deviation of the exponent from the ideal value of 3/2 is observed, (see figure 3). Increasing the number of layers of the unit cell, the gaps become smaller and their influence over

the parabolic form of the bands is smaller; as a result of this the exponent is more similar to 3/2.

3.1.2. Strong coupling. The limit of strong coupling between two consecutive magnetic films is simulated by using a value of $J_I = 2 \times 10^{-15}$ erg, very near to the value of J. The results are shown in figure 4. In this case the thermal behaviour of the magnetization is almost independent of the number of monatomic layers of the unit cell and the exponent of the $T^{3/2}$ power law is 1.53 in all cases (see figure 3). This small deviation with respect to the value of 3/2 can be explained by taking into account the variation of the quadratic dispersion relation arising from the presence of gaps generated by the periodic structure. Thus we observe that the strength of J_I controls the thermal behaviour of the magnetization of the superlattice system leading to a very important dependence on the layer thickness in the weak-coupling limit or a behaviour that is independent of layer thickness in the strong-coupling limit. To understand this we need to take into account the features of the superlattice magnon spectrum.

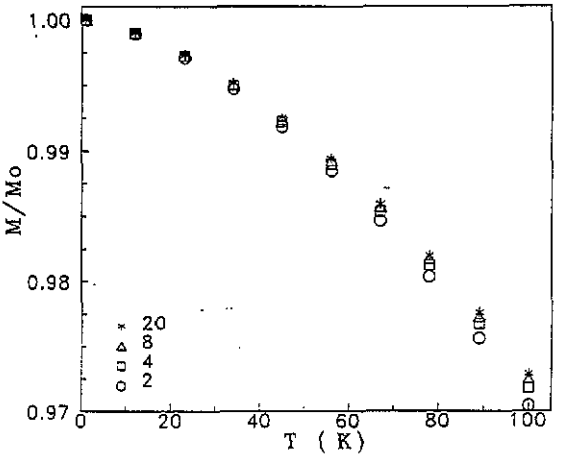

Figure 4. Thermal behaviour of the magnetization as a function of the thickness of the unit cell (in monatomic layers). The value of J_I is 2×10^{-15} erg and the external applied field is zero.

Physically the collective modes of the superlattice result from the superposition of individual film modes. When J_I is small the resulting superlattice modes form very narrow bands and we have nearly discrete levels similar to that of an isolated film. As the strength of the coupling at the interfaces increases, the superlattice bands broaden. Finally when J_I is similar in size to J, the broadening of the bands leads to a quasi-continuous band similar to those in bulk materials. Thus in the weak-coupling limit one has a set of states similar to that of a single film, while in the strong-coupling limit one has a set of energy levels which is close to that of a bulk material. This explains the strong dependence on the layer thickness in the weak-coupling limit since the smaller the number of layers in a unit cell, the larger the separation between the energy levels, and the quasi-bidimensional behaviour is more evident.

3.1.3. Effects of the external applied field. The immediate effect of a magnetic field is the introduction of an energy gap into the spin wave spectrum. The effect of the

applied field on the thermal behaviour of the magnetization is presented in figure 5. As the magnetic field is increased, a slower decrease of the magnetization is observed. Furthermore, we have found that the effect of the magnetic field increases as the number of monatomic layers of the unit cell decreases. The effect is more important when the intensity of the field increases because the gap generated in the magnon spectrum is proportional to the size of the field, $\Delta E = g\mu_B H$.

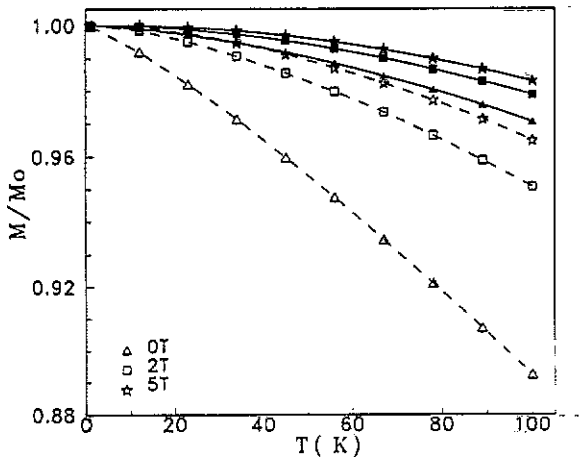

Figure 5. Thermal behaviour of the magnetization for the unit cell with two monatomic layers as a function of the intensity of the external applied field (0, 2 and 5 T). The full curves and full symbols indicate strong coupling and the broken curves indicate weak coupling.

It is also observed that the effect is more important in the case of weak coupling. The addition of a magnetic field produces an exponential variation of $M(T)$ in the low-temperature regime but an asymptotic behaviour indicating a $\Delta M/M \propto T^{\alpha}$ type of dependence is observed in the high-T regime with an exponent α clearly larger than 3/2 (figure 6).

3.2. System of two different ferromagnetic materials

We now turn to the results for a system of two different ferromagnetic materials that interact ferromagnetically at the interfaces. Some preliminary results for this system have been published in ICM'88 proceedings [18].

For the purposes of numerical calculations material 1 will be considered to have a moment $S_1 = \frac{3}{2}$ while material 2 will have a moment $S_2 = \frac{5}{2}$. The corresponding values for the exchange integrals will be $J_1 = 14.19 \times 10^{-16}$ and $J_2 = 27.6 \times 10^{-16}$ erg.

As in the preceding case this study has been performed as a function of the interface coupling strength, the number of monatomic layers of the unit cell and the intensity of the external applied field.

3.2.1. Weak coupling. The limit of weak coupling at the interfaces has been simulated by taking $J_1 = 10^{-16}$ erg. In figure 7 we show the thermal behaviour of the magnetization as a function of the number of monatomic layers in the unit cell. Clearly the magnetization decreases faster as the number of layers of the unit cell decreases. This

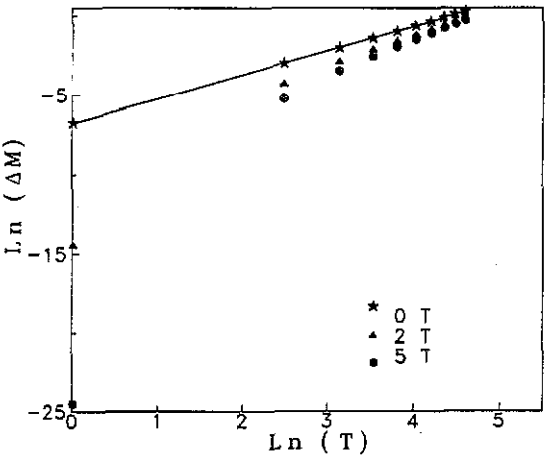

Figure 6. Determination of the exponent of the '$T^{3/2}$ power law' for the 20 monatomic layer unit cell. Data obtained with external applied fields of 2 T (▲) and 5 T (●) are also shown making evident the departure of the power law owing to the effect of the field.

type of behaviour is similar to that we found in the first system studied. On the other hand, when we try to characterize this type of behaviour in terms of the $T^{3/2}$ power law we observe that the values for the exponent vary between 1.54 for the 'thinnest cell' (2/2 monatomic layers) and 1.51 for the 'thickest cell' (20/20 monatomic layers). The small deviation with respect to the value of 3/2 could be explained by taking into account the small variation of the quadratic dispersion relation introduced by the energy gaps owing to the periodicity of the superlattice.

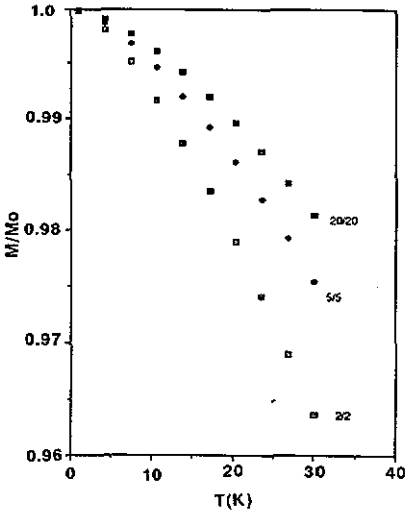

Figure 7. Thermal behaviour of the magnetization as a function of the thickness of the unit cell for system 2 in the weak-coupling limit for $H = 0$ T.

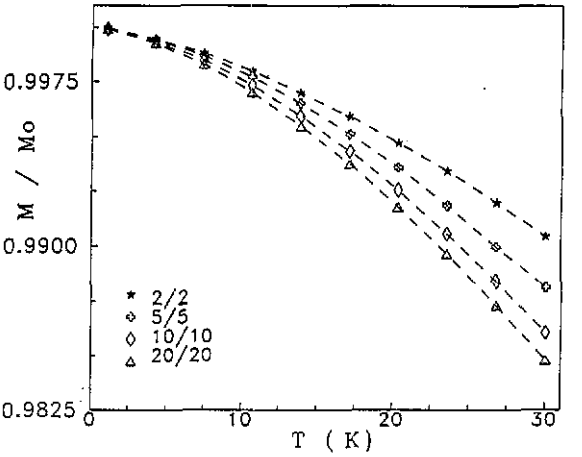

Figure 8. Thermal behaviour of the magnetization as a function of the thickness of the unit cell for system 2 in the strong-coupling limit for $H = 0$ T.

3.2.2. Strong coupling. In the case of strong coupling the value assigned to J_I was

$J_1 = J_2$. The decrease of the magnetization with temperature as a function of the number of monatomic layers of the unit cell is shown in figure 8. A very intriguing type of behaviour is found in this case since the magnetization decreases faster as the number of monatomic layers of the unit cell increases. This type of behaviour is opposite to that observed for the weak-coupling case. To understand this we note that $M(T)$ tends towards the bulk behaviour of the material with the lower Curie temperature as the number of monatomic layers of the unit cell is increased. In the weak-coupling limit the value of D_{eff} is smaller for thinner layers (where the interface coupling is important) and then increases for thicker layers (nearing the bulk behaviour). This leads to the more rapid decrease in the magnetization with temperature seen for a smaller number of layers in figure 7. The opposite occurs in the strong-coupling limit.

Explicit examples of the superlattice magnon spectrum are presented in figure 9 for both the weak-coupling limit (figure 9(*a*)) and the strong-coupling limit (figure 9(*b*)). Here we plot the frequency as a function of the wavevector perpendicular to the layers. In figure 9(*a*) we see distinctly the 'softer' value of D_{eff} for a system with a smaller number of layers in a unit cell, that is the curvature near $q = 0$ is smallest for the 2/2 structure. In contrast figure 9(*b*) shows that in the strong-coupling limit the curvature is smallest for the 10/10 structure. In both the strong- and weak-coupling limits we see the gaps introduced by the superlattice periodicity. When comparing the thermal response of the strong- and the weak-coupling limits, one must remember that the excitation energies for the weak-coupling case are significantly smaller than for the strong-coupling case.

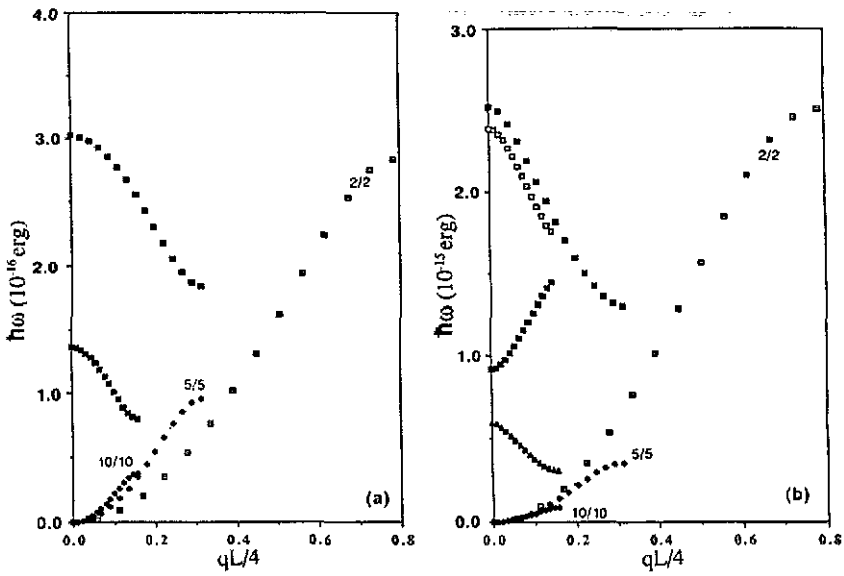

Figure 9. Comparison of the first magnon bands as a function of the thickness of the unit cell: (*a*), weak-coupling limit; (*b*), strong-coupling limit. Some bands are shown in the reduced-zone scheme.

As mentioned earlier the band gaps introduced by the periodic structure of the superlattice (figure 9) should allow deviations from the $T^{3/2}$ power law. In the temperature range from 1 to 30 K the values found for the exponent in this case vary

between 1.58 for the (20/20) sample and 1.51 for the (2/2) sample.

As we mentioned when we discussed the results of the first system the immediate effect of a magnetic field is the introduction of an energy gap into the spin wave spectrum. In figure 10 we show the behaviour of the magnetization as a function of the intensity of the external applied field. A slower decrease of the magnetization with temperature is observed.

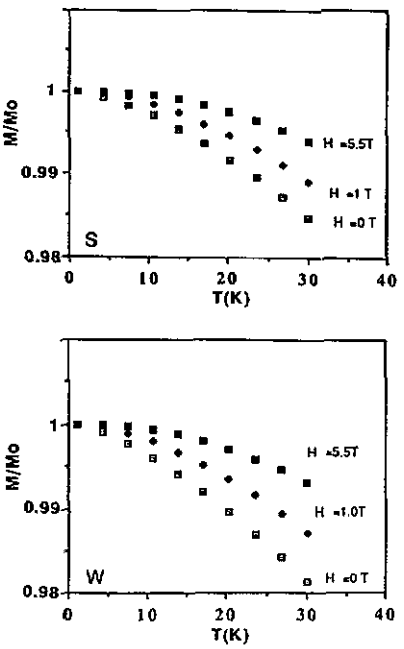

Figure 10. Effect of the external applied field on the thermal behaviour of the magnetization for the 20/20 monatomic layers sample in the cases of strong (S) and weak (W) coupling.

4. Conclusions

We have studied the spin wave spectrum of the two systems, the first composed of alternating films of ferromagnetic and non-magnetic materials and the second of alternating films of two different ferromagnetic materials. In both cases the study has been performed as a function of the applied field, the number of monatomic layers in the unit cell and the intensity of the interaction in the interface of the different materials.

For the first system a clear tendency to a bidimensional type of behaviour is found when the exchange coupling at the interface is very small ($J_I \ll J$). When J_I is very small the successive films of the magnetic material are almost isolated one from each other and the thermal behaviour of the magnetization shows a clear dependence on the number of monatomic layers of the unit cell. On the contrary when J_I is very similar to J the dimensional effects disappear and what we get is a variation of the spin wave stiffness constant D_{eff}. This variation arises from the dependence of D_{eff} on J and J_I. The role of J_I increases when the unit cell becomes thinner.

In the case of the second system we again observe that the exchange coupling at the interface of both materials plays an important role and is the parameter that

governs the thermal behaviour of the magnetization. $M(T)$ tends towards the bulk behaviour of the material with the lower Curie temperature as the unit cell becomes thicker. In the weak-coupling limit the role of J_1 is more important as the unit cell becomes thinner. Thus the value of D_{eff} decreases leading to a more rapid decrease of the magnetization with temperature for thinner unit cells. In the limit of strong coupling the opposite type of behaviour is observed.

In the study of both systems we have observed that the application of an external magnetic field has an important influence in the thermal behaviour of the magnetization of the system, making the variations of M significantly smaller.

A near exponential dependence is observed for $M(T)$ in the low-T regime but an asymptotic behaviour indicating a $\Delta M/M \propto T^{\alpha}$ type of dependence is observed in the high-T regime with a value of α clearly different from 3/2.

Acknowledgment

The work of REC was supported by the US Army Research Office, grant No DAAL03-88-K-0061.

References

[1] Gyorgy E M, Mcwhan D B, Dillon J F, Walker L R, Waszczak J V, Müuser D P and Willies R H 1983 *J. Magn. Magn. Mater.* **31–4** 915
[2] Hosoito N, Kawaguchi K, Shinto T, Takada T and Endoh Y 1984 *J. Phys. Soc. Japan* **53** 257
[3] Martínez B, Moreu M A, Labarta A, Obradors X and Tejada J 1988 *J. Appl. Phys.* **63** 3206
[4] Gavrin A, Childress J R, Chien C L, Martínez B and Salamon M B 1990 *Phys. Rev. Lett.* **64** 2438
[5] Grünberg P and Mika K 1983 *Phys. Rev.* B **27** 2955
[6] Camley R E, Rahmam T S and Mills D L 1983 *Phys. Rev.* B **27** 261
[7] Camley R E 1984 *J. Physique Coll. Suppl.* **45** C5 315
[8] Camley R E and Cottam M G 1987 *Phys. Rev.* B **35** 189
[9] Albuquerque E L, Fulco P, Sarmento E M and Tilley D R 1986 *Solid State Commun.* **58** 41
[10] Dobrzynski L, Djafari-Rouhami B and Puszkarski H 1986 *Phys. Rev.* B **33** 3521
[11] Morkowski J A and Szajek A 1988 *J. Magn. Magn. Mater.* **71** 299
[12] Schwenk D, Fishman F and Schwabl F 1988 *Phys. Rev.* B **38** 11 618
[13] Holstein T and Primakoff H 1940 *Phys. Rev.* **58** 1098
[14] Kittel C 1987 *Quantum Theory of Solids* (New York: Wiley) ch 4
[15] Keffer F 1966 *Handb. Phys.* vol 18 (Berlin: Springer)
[16] Klein M J and Smit R S 1951 *Phys. Rev.* **81** 378
[17] Bruno P 1991 *Phys. Rev.* B **43** 6015
[18] Camley R E, Martínez B and Lepage J G 1988 *J. Physique Coll.* **49** C8 1691